Scanning Microscopy

Volume 1993
Number 7 *Physics of Generation and Detection of Signals Used for Microcharacterization*

Article 6

1993

Influence of Primary Electron Beam Angle of Incidence on Auger Electron Spectra

Mark A. Smith
University of Cincinnati

Scanning Microscopy Supplement 7, 1993 (Pages 49-56) 08921-953X/93$5.00+.25
Scanning Microscopy International, Chicago (AMF O'Hare), IL 60666 USA

INFLUENCE OF PRIMARY ELECTRON BEAM ANGLE OF INCIDENCE ON AUGER ELECTRON SPECTRA

Mark A. Smith*

Department of Chemistry, ML 172, University of Cincinnati
Cincinnati, OH 45221-0172, USA
Phone Number: (513) 559-1176

Abstract

A principal step in the extraction of Auger electron yields and line shapes from electron-excited spectra is an understanding of the attendant electron background. Experiments are reported here in which the influence of the primary electron beam angle of incidence on Auger spectral backgrounds has been separated from that of the angle of electron emission. The secondary electron background for clean polycrystalline palladium, on the high-energy side of the MNN peaks, have been studied as functions of primary beam angle of incidence and beam energy. For the range of beam energies investigated, < 10 keV, linearization of the secondary cascade is easily observed in log-log plots of intensity versus energy. When cascades are fitted with Sickafus-type functions, AE^{-m} (E = electron energy), the parameter m is found to depend on the beam angle of incidence but not on the beam energy. The effect of increasing primary beam energy is to enlarge the energy interval over which linearization can be observed. The low-energy inelastic "step" or "tail" accompanying the background-subtracted Auger peaks grows in intensity as the angle of incidence approaches that of the surface normal.

Key Words: Auger electron spectroscopy (AES), secondary electron cascade, backscattered primary electrons, quantitative AES, electron background removal, primary beam angle of incidence, angle of electron emission, secondary cascade linearization, electron beam micro-analysis, shape of Auger electron spectra.

*Current address for correspondence:
Mark A. Smith,
5306 Indiana St.,
Apt. 11,
South Carleston, WV 25309

Introduction

Methods for quantifying electron-excited Auger electron spectroscopy (AES) treat data acquired in one of two ways: in the traditional, "derivative" mode (dN/dE, where N is the electron distribution, and E is the electron energy) or in the direct or "integral" mode (N(E)). The principal advantage of using the derivative mode is the easy suppression of the large slowly varying electron background upon which the features of interest, the Auger peaks, rest. Two advantages of using the integral mode are of direct interest to those engaged in microbeam analysis. The first advantage is that electron beams with the size to probe features tens of nanometers in extent will usually produce Auger electron yields too small for clear recognition with lock-in/modulation-based derivative schemes or with computer differentiation of pulse-counting detection; the signal-to-noise ratio should be superior in the integral mode. The second advantage is the opportunity to obtain information about subsurface species. As first discussed by Sickafus (1977a, 1977b), detection of subsurface elemental concentrations and relative locations should be possible in the integral mode. Realization of this possibility poses enormous difficulties.

Inherent in extracting surface and subsurface Auger yields is the challenge of characterizing the electron background attendant to the Auger peaks so that an unarbitrary method for subtracting out well understood sources of non-Auger electrons can be developed. This paper deals with one aspect of characterizing the electron background present in Auger N(E) spectra — the influence of the primary electron beam angle of incidence upon the shape of the spectra.

Review of Previous Work

The first systematic study of the angular dependence of the background (of N(E)-mode AES) was done by Sickafus (1977a). Working with a model of the secondary electron cascade based on the Boltzmann diffusion equation, Sickafus postulated that regions of the electron spectrum would be linear in plots of lnN versus lnE;

sections of the cascade on the high-energy side of an Auger threshold could be fitted with functions of the form AE^{-m}, where A is a constant and m is the slope observed in the log-log plots. In reporting his observations of linearized sections of the secondary cascade for Ni(110), he also plotted the slopes of the linear sections as a function of the angle of rotation of his sample with respect to the electron gun used for excitation. Sickafus found that the slopes of the linear segments decreased as the angle of electron beam incidence approached the surface normal.

Obtaining a clearer view of angular dependence in Sickafus' data is hampered by two factors: the use of a retarding field analyzer, which averages over large angles of emission; and the use of a 3 keV primary beam energy, for which the contribution of backscattered primaries in the range of analytical interest, $E \leq 2000$ eV, should be great enough to hinder clear observation of the secondary cascade at energies above ~500 eV.

Other groups have investigated the dependence of the electron background upon the angle of electron beam incidence. Peacock (1985) has measured m, the slope of the cascade (using the Sickafus model), for select energy regions of Ag and InP specimens, as a function of incident beam angle. He showed a variation of m from ~0.65 to ~0.9 as the angle of incidence was increased from 0° to ~75°, for Ag in the energy range of 400-500 eV. Peacock and Duraud (1986) published work detailing the observational conditions for linearization of the background in log-log plots of spectra. They found observed background could be expressed as a sum of two power functions of electron energy, AE^{-m} and BE^{n}, where B is a constant. The first term describes a Sickafus-type approximation to the secondary cascade, but m in this case is not necessarily the empirically measured slope; the second term is an approximation to the contribution of backscattered primaries. This paper did not address the angular dependence of the parameters found in the power-law expressions.

Work by Matthew *et al.* (1988) demonstrated that cascade linearization could be observed over large regions of electron energy (up to 2000 eV) for sufficiently high primary beam energies, i.e., up to 23 keV, for a variety of materials. Their work, however, did not address the dependence of the cascade upon beam angle of incidence.

In early work, Bishop (1982, 1983) measured Auger electron spectra in the EN(E) mode for a number of different materials over a wide range of incident beam angles; he did not attempt to characterize the functional form of the secondary cascade or show how the cascade depended on the angle of incidence. In later work, however, Bishop, with collaborators Batchelor and Venables (Batchelor *et al.*, 1989), demonstrated with spectra taken for Cu that the electron background depends on both the angle of incidence and the primary beam energy. In particular, they found that the contribution of the backscattered primaries decreases with increasing angle of incidence. They also showed that backscattered primaries make a smaller contribution to the electron background as the primary beam energy increases up to ~15 keV; above 15 keV, the slope of the spectra remains unchanged from that at 15 keV, and the background above the Cu peaks appears to be straight. Although they presented their data in the EN(E) form, and thus could not demonstrate secondary cascade linearization, it can be deduced from their spectra that observation of cascade linearization should be most feasible at higher angles of incidence and at higher primary beam energies. This is demonstrated most effectively in their spectra for primary beam energies greater than 15 keV; the straight spectral backgrounds above 1000 eV in the EN(E) mode indicate that the same spectra replotted in the N(E) form would have backgrounds above 1000 eV with the functional form of E^{-1}.

Scope of this Work

This paper has two objectives. The first is to present some limited data on the dependence of the electron background upon the angle of emission, θ. These data have been obtained for a select set of experimental parameters, from several materials, e.g., alumina and iron. The general trend observed in these measurements will be contrasted with that seen for the dependence of the background on the angle of primary beam incidence, α. The second objective is to present measurements obtained from polycrystalline palladium which show the behavior of the secondary cascade as a function of α. The range of primary beam energy, E_p, reported here, varies from 4 keV to 10 keV. For primary energies greater than 4 keV, linearization of the secondary cascade can be observed above the MVV transition of palladium ($E > \sim 530$ eV). The electron background at energies greater than this transition are free of Auger peaks up to 2000 eV — for clean samples. This peak-free interval ($530 \text{ eV} < E < 2000 \text{ eV}$) allows for a clear inspection of the apparent transition of the spectral background from a region dominated by the secondary cascade to one dominated by the backscattered primaries.

A special note should be made of the experimental conditions which have been chosen. The intent of this study was to examine cascade behavior uncomplicated by effects, caused by diffraction or other processes, seen in spectral data collected with analyzers of high angular resolution and/or with single-crystal specimens. Conse-

quently, polycrystalline samples were selected. An analyzer with an angular resolution better than those of retarding-field devices and most cylindrical mirror analyzers was used to probe the θ-dependence of the spectral background (see the following section).

Materials and Methods

Since the experimental system used for this study has been described in detail elsewhere (Smith, 1991), only major aspects will be given here. All measurements were carried out in a well magnetically shielded ultrahigh vacuum system; except during sample cleaning with Ar ion bombardment, pressures below 1 x 10^{-8} Pa were maintained. Electron spectra were acquired with a Leybold-Heraeus EA10/100 spectrometer. Auger spectra were measured in the integral EN(E) mode, with $\Delta E/E$ constant (B=3) and with pulse counting. The plateau of the intensity-bias voltage curve of the electron multiplier (18-dynode venetian-blind type) was determined by monitoring the intensity of the MVV peak of copper (at ~60 eV). Spectra were acquired and digitized with a Tracor Northern TN1710 system and were then transferred to a Macintosh II personal computer for data processing and plotting. Each measured spectrum was corrected for electron multiplier response and the spectrometer transfer function in the computer to yield the energy distribution N(E). The angle of acceptance of the spectrometer in the plane perpendicular to the axis of sample rotation was 9°.

The cylindrical experimental chamber was mounted vertically; a port at the center of the top of the chamber was used for mounting the sample manipulator. The manipulator allowed for 360-degree rotation of the sample, the surface of investigation of which was aligned with the chamber's axis. The input end of the electron spectrometer pointed radially inward at the sample.

Two electron guns, one fixed in position and one rotatable, were used for spectral excitation. For either gun, electron beam currents ranged between 2 and 10 nA. Beams delivered by the rotatable gun were focussed to spots approximately 0.5 mm; beam spot size for the fixed gun ranged between 5 and 10 μm. The fixed gun was mounted on a port 60° away from the spectrometer port in a horizontal plane that included the normal to the sample and the spectrometer input-axis. When used with the fixed gun, rotation of the sample provided for the variation of the incident beam angle, α, with a concomitant variation of the electron emission angle, θ. Primary beam energies up to 10 keV could be attained with this gun.

The rotatable electron gun was mounted on a frame which could revolve about the axis of the vacuum chamber, with the gun always pointing at the same spot on the sample, regardless of whether the sample or the gun were rotated. This gun lay below the spectrometer input lens-axis, pointing up at the sample. The axis of the gun was co-planar with the chamber-axis; when the axis of the gun and the normal to the sample's surface were made co-planar, the angle of incidence of the electron beam from the gun was 60° with respect to the normal. The angle of incidence could be made larger by rotating the sample or the electron gun so that the gun-axis was not co-planar with the normal to the sample. Thus, it was possible with the rotatable gun to perform experiments in which the angle of incidence was held fixed ($60° \leq \alpha < 90°$) while the angle of emission could be varied from zero to ~90°. Each time the sample was rotated through a specified angle (changing θ) the gun was rotated the same amount (keeping α fixed). This gun could deliver beam energies up to 5 keV.

The samples used for this study consisted of thin polycrystalline foils of palladium and iron and thin wafers of stress-annealed pyrolytic graphite and polycrystalline alumina. The purity of each material was rated at 99.99% or better, and the average grain size of the polycrystalline specimens was smaller than 0.01 mm. Samples were cleaned by sputtering and annealing until no contaminants could be detected in the Auger spectra for Pd or until small peaks for carbon and oxygen were reduced to the smallest attainable values for Fe and alumina.

Results

The dependence of the electron background on θ was investigated (using the rotatable gun) over a narrow range of experimental parameters. Generally, the shape of the spectral background can vary considerably for some materials at primary beam energies lower than ~4 keV. For example, in Figure 1 are shown two N(E) spectra for polycrystalline alumina which were generated with primary beams of energy of 1.95 keV and angle of incidence of 60°; the spectra were scaled so that the peaks corresponding to elastically scattered primaries were of the same intensity. Clearly the shapes of the backgrounds differ dramatically.

At higher values of primary energy, e.g., > 5 keV, spectral backgrounds appear to have the same basic shape, independent of emission angle. Figure 2 shows EN(E) spectra acquired, again for alumina, with the angle of emission varying from 0 to 60°; the primary beam was incident at an angle of 60°, at 5 keV. The spectra have been scaled to make the intensities of the high-energy alumina peaks the same value; the zero-points of the intensity axes have been shifted for clarity of display. Figure 3 plots EN(E) spectra obtained for polycrystalline iron at different angles of emission for

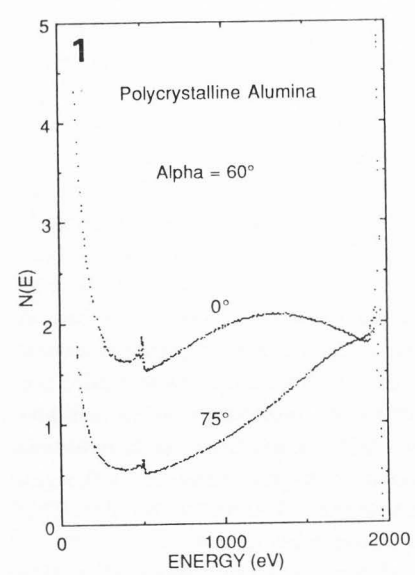

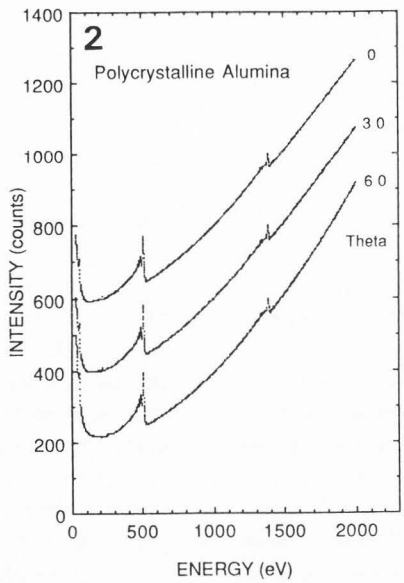

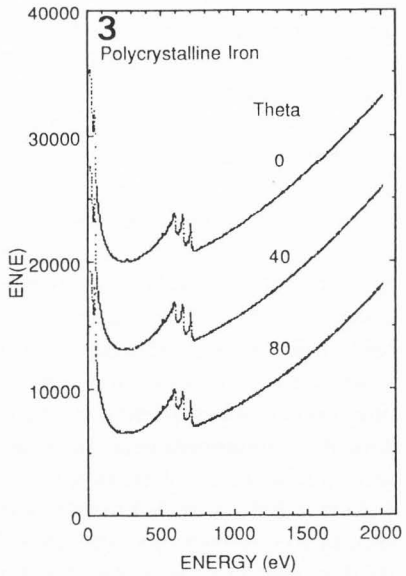

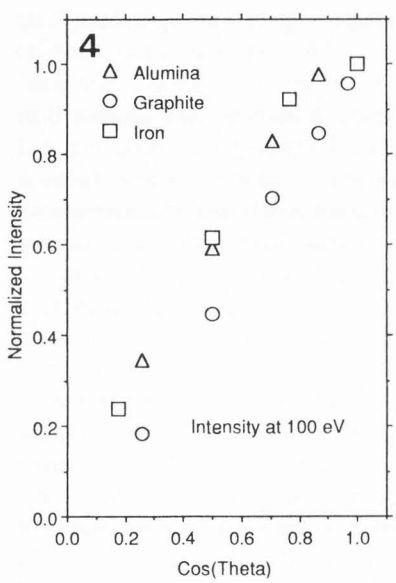

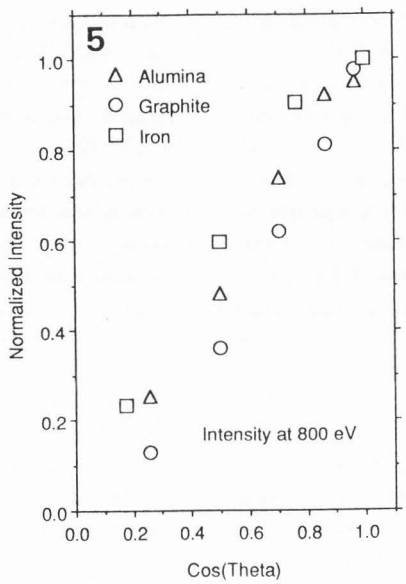

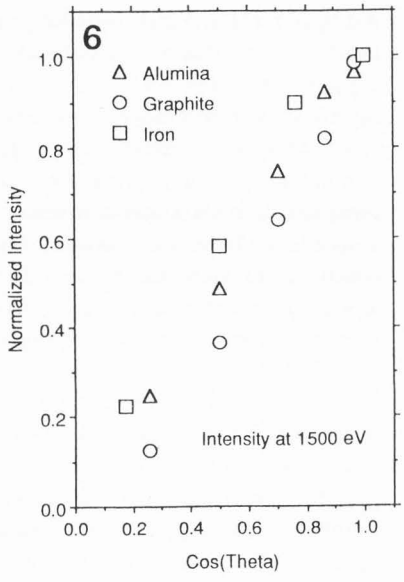

Figure 1 (above left). N(E) spectra for polycrystalline alumina acquired with a primary beam energy of 1.95 keV and an angle of incidence of 60°. The numbers above the curves indicate the angle of emission at which the spectra were recorded. The spectra have been scaled so that the elastic peak maxima are of the same intensity.

Figure 2 (above center). EN(E) spectra for polycrystalline alumina acquired with a primary beam energy of 5 keV and an angle of incidence of 60°. The angle of emission is indicated for each curve. The spectra have been scaled to make the intensities of the high-energy aluminum peaks the same value; the zero-points of the intensity axes have been shifted for clarity of display.

Figure 3 (above right). EN(E) spectra for polycrystalline iron; the primary beam energy was 5 keV, and the angle of incidence was 60°. The angle of emission is indicated for each curve. The spectra have been scaled and shifted in a manner similar to that of Figure 2.

Figure 4 (below left). Normalized intensity at 100 eV versus the cosine of the angle of emission for graphite, iron and alumina. The plotted values are the measured intensities divided by the associated beam current and then normalized by the value for $\theta = 0°$.

Figure 5 (opposite, below center). Normalized intensity at 800 eV versus the cosine of the angle of emission for graphite, iron and alumina. The plotted values are the measured intensities divided by the associated beam current and then normalized by the value for $\theta = 0°$.

Figure 6 (opposite, below right). Normalized intensity at 1500 eV versus the cosine of the angle of emission for graphite, iron and alumina. The plotted values are the measured intensities divided by the associated beam current and then normalized by the value for $\theta = 0°$.

$E_p = 5$ keV and $\alpha = 60°$ (these spectra have been scaled and shifted in a way similar to that of Figure 2). The similarity of background shapes is striking, indicating that at sufficiently high primary beam energy θ does not influence the shape of the Auger spectrum significantly.

The dominant effect that has been masked in Figures 1-3 is the decrease in intensity, at all energies, as θ increases. One would expect, from purely geometric considerations (given a constant primary beam current), the background intensity at any energy to follow a cosine function of θ. This adherence to a cosine-type behavior was observed for materials such as iron, alumina and graphite when E_p was 5 keV and α was 60°. Figures 4, 5 and 6 display the plots of normalized spectral intensity at energies of 100, 800, and 1500 eV, respectively, as a function of $\cos\theta$; the plotted values are the experimentally measured intensities divided by the associated beam current and then normalized by the value for $\theta = 0°$.

The dependence of the electron background upon α is much stronger than that of θ. This dependence can be seen in Figure 7, where spectra obtained for $\alpha = 0°$ and 80° are compared. The influence of the angle of incidence has been studied (using the fixed electron gun) by measuring N(E) spectra over the energy range of 50 to 2000 eV, for E ranging from 4 keV to 10 keV, for α equal to 0, 15, 30, 40, 50, 60, 70 and 80 degrees. When these spectra are replotted as lnN versus lnE, several observations about the secondary cascade can be made: (**1**) For each α, linearized sections of the cascade can be seen starting at ~530 eV and extending upwards in energy when the primary beam energy is sufficiently high, that is, > 6 keV; (**2**) the extent in energy of the linear sections depends directly on the primary beam energy; and (**3**) when fitted to functions of the type AE^{-m} the linear sections have values of m dependent on α but independent of E_p.

An example of these observations is given in Figure 8. In the figure, the data are displayed between lnE = 6.1 and 7.2; the linear sections can be seen to start at 6.27 (as indicated by the leftmost arrows). Arrows below the spectra at higher energies indicate the upper limit for which the slope of the linear region does not vary more than 5% from the average value over the region. Each curve corresponds to a value of E_p. The measured value of m for each linear region is fairly constant as E_p varies; this result was found to occur for each α.

Figure 9 shows a plot of m (an average value obtained from spectra taken at several values of E_p) versus α. The parameter m appears to be constant for $\alpha <$ 40°, but significant variation occurs above 40°. A comparable trend for the parameter A is shown in Figure 10. In this figure, the plotted values of A have been normalized by their respective peak heights for the

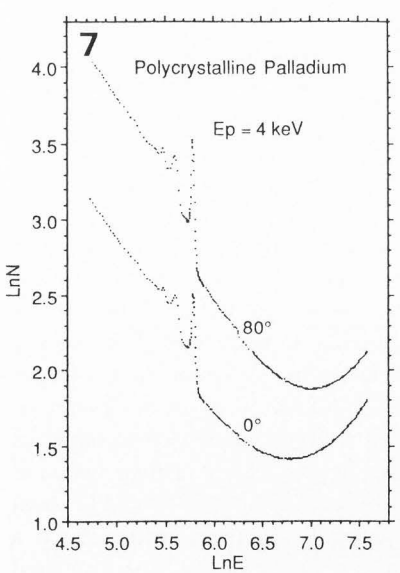

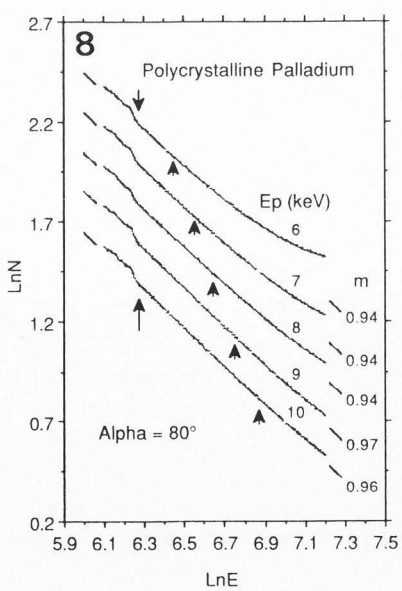

Figure 7 (left). Comparison of spectra acquired for palladium at angles of incidence of 0° and 80°, for E_p=4 keV.

Figure 8 (right). Comparison of spectra acquired for palladium at an angle of incidence of 80°, at primary beam energies of 6, 7, 8, 9 and 10 keV. The energy region of the plot has been chosen to display clearly the sections of linearized cascade present for each spectrum. The arrows denote the limits of the observed linear regions. The short line segments to the upper left and lower right of each spectrum have been included to aid in viewing the linear sections. The fitted values of m have also been specified.

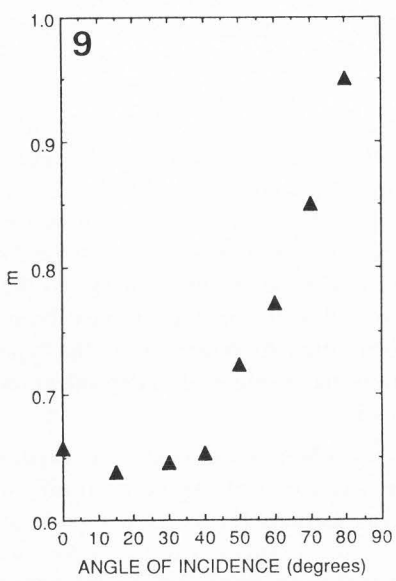

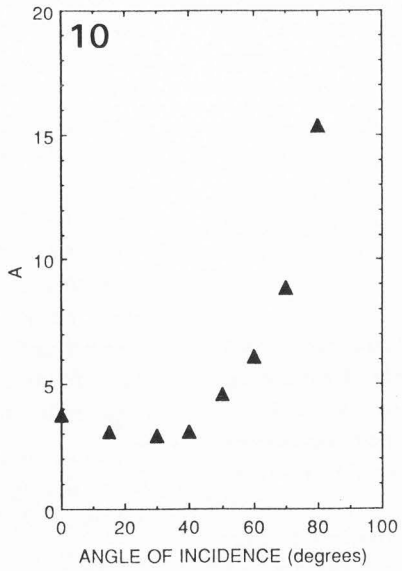

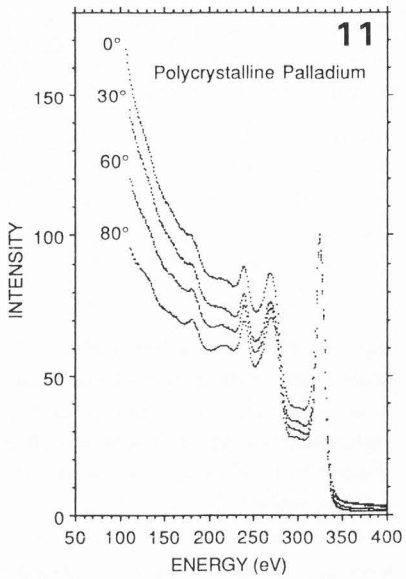

Figure 9 (left). Plot of cascade parameter m versus the angle of beam incidence. The values shown are averages obtained from measured values of m taken at several primary beam energies. Data are for polycrystalline palladium.

Figure 10 (center). Plot of the cascade parameter A versus the angle of beam incidence. Plotted values are averages and have been normalized by respective peak heights for the MNN transition at 323 eV, after the cascade background has been subtracted. Data are for polycrystalline palladium.

Figure 11 (right). The MNN Auger spectra of palladium after removal of the linearized cascade, acquired at different angles of incidence. The spectra are averages of spectra taken at various values of primary beam energy. All curves have been scaled to make the peak height at 323 eV equal to 100.

MNN transition at 323 eV, after the cascade background has been subtracted.

It is evident in Figure 8 that for $\alpha = 80°$ and $E_p =$ 10 keV the contribution to the electron background by backscattered primaries is quite small. For decreasing E_p, however, the deviation from linearity becomes greater, an indication of the increasing contribution from backscattered primaries. It seems reasonable to conjecture that the smaller values of m seen at lower values of α result from the sum of the secondary cascade and the backscattered primaries in such a way that the cascade part is the dominant component but that the backscattered part moderates expression of the cascade. It is hoped that further analysis of these data will yield information about the backscattered component of the background. Knowledge of the backscattered primaries is required to do a better job of background removal than is currently available with the Sickafus approximation.

When one uses the measured values of A and m to subtract the cascade contribution from the palladium Auger spectrum one obtains a spectrum that exhibits a low-energy "step" or "tail" that increases in intensity with decreasing electron energy. This step arises principally from inelastic losses suffered by Auger electrons escaping from regions of the sample where the probability of inelastic loss is significant. Figure 11 shows the Auger spectra of palladium for different values of a after subtraction of the cascade has been done; the plotted data are averages of the spectra taken for each value of E_p where linearization was observed — each individual spectrum agrees in shape very well overall with the other spectra with which it was averaged.

Clearly, the low-energy step varies (at any given energy below the most prominent Auger peak) in intensity with α. A similar result was obtained for Ag by Peacock (1985). The increase in intensity of the step as α approaches zero is most likely the result of deeper penetration of the incident electron beam at smaller α, causing to be generated a larger number of secondaries associated with the Auger peak. Any method which is devised for removal of the inelastic step should account for the influence of α on the step intensity. Such a method is currently being sought and will be discussed in future papers.

Discussion

Linearization of the secondary electron cascade (in log-log plots), for E > 530 eV, has been observed for polycrystalline Pd for all angles of the incident primary beam and for beam energies of 6 keV and greater. In this regime of primary beam energy, the effect of emission angle upon spectral shape was found to be minimal. Other than choice of E_p, the beam angle of incidence has the greater influence on the shape of the electron background. The negative slope of the linearized cascade varies with α, and reaches a maximum close to one. The extent in energy over which cascade linearity is observed depends on α and E_p. Upon removal of the cascade component of the background, the palladium Auger spectrum displays an inelastic-loss step at lower energy which varies in intensity with the angle of incidence. Proper removal of this step will require a method which takes the angular effect into account. It is anticipated that further analysis of the angular dependent spectra will provide insight into the behavior of the backscattered primaries.

Acknowledgments

The experimental part of this work was carried out at the Union Carbide Technical Center, South Charleston, West Virginia.

References

Batchelor DR, Bishop HE, Venables JA (1989) Auger electron spectroscopy from elemental standards. III. Backgrounds and peak-to-background ratios. Surf. Interface Anal. **14**, 709-716.

Bishop HE (1982) The role of the background in Auger electron spectroscopy. In: Electron Beam Interactions with Solids. Kyser DF, Niedrig H, Newbury DE, Shimizu R (eds.). SEM Inc., O'Hare, IL, 259-269.

Bishop HE (1983) Background intensity signal normalisation in Auger electron spectroscopy. Scanning Electron Microsc. **1983**;III, 1083-1090.

Matthew JAD, Prutton M, El Gomati MM, and Peacock DC (1988) The spectral background in electron excited Auger electron spectroscopy. Surf. Interface Anal. **11**, 173-181.

Peacock DC (1985) Fitting the inelastic tail below experimentally observed Auger peaks. Surf. Sci. **152/153**, 895-901.

Peacock DC, Duraud JP (1986) The shape of the background in AES: Nonlinear features in logN(E) v. LogE. Surf Interface Anal. **8**, 1-6.

Sickafus EN (1977a) Linearized secondary-electron cascades from the surfaces of metals. I. Clean surfaces of homogeneous specimens. Phys. Rev. B **16**, 1436-1447.

Sickafus EN (1977b) Linearized secondary-electron cascades from the surfaces of metals. II. Surface and subsurface sources. Phys. Rev. B **16**, 1448-1458.

Smith MA (1991) Instrumental considerations for acquiring quantitative Auger electron spectra. J. Vac. Sci. Technol. A **9**, 2309-2314.

Discussion with Reviewers

R. Shimizu: You stated that Peacock and Duraud were able to fit observed electron backgrounds with a sum of two functions, AE^{-m} and BE^{n}. Have you tried to do this with spectra of polycrystalline palladium? It would be very helpful to show plots similar to Figures 9 & 10 for B and n.

Author: The primary intent of this paper was to demonstrate that linearized secondary cascade behavior could be observed at all angles of incidence for sufficiently high primary beam energy. The presentation of data in Figures 8-11 has been based on a Sickafus-type approach to modelling the secondary background as a starting point for studying the parameters affecting spectral backgrounds. It is the author's opinion that the Sickafus model is too simplistic and that the model of Peacock and Duraud represents a more general approach. Work is currently underway to analyze the palladium spectra according to their model.

R. Shimizu: Why did you not choose aluminum or silicon instead of alumina to compare with theoretical (Ding ZJ, Shimizu R (1988) Surf. Sci. **197**, 539-554) and experimental (Bishop, 1982) investigations?

Author: Alumina was chosen for study because of its electrical conductivity. The choices of iron, graphite and alumina were made to obtain data from representatives of the categories metal, semiconductor (or semimetal), and insulator, respectively. Perhaps silicon should have been selected instead of graphite, but graphite was readily available at the time of this study and was needed for another investigation.

H. Bishop: How is the interpretation of your results complicated by the fact that the take-off angle is different for the different incident angles?

Author: Although the effects of incident angle and take-off angle have not been thoroughly disentangled in this work, the data shown in Figures 2 & 3 indicate a trend: At an incident angle of 60° the **shape** of the electron spectra does not change regardless of take-off angle. A similar result was found for an incident angle of 80°. Since the effects of backscattered electrons are more pronounced at smaller values of incident angle it

is possible that spectral shapes will not be independent of take-off angle at incident angles less than 60°. The result of this study, however, is that spectral shapes are independent of take-off angle for incident angles > 60°.

H. Bishop: The transmission function of the analyzer should be established if the value of m is to have any meaning in comparison with other instruments. Seah and co-workers have published a reference spectrum for copper that allows the transmission function to determined.

Author: The properties of the analyzer used in this study have been described in detail in a paper (Smith, 1991) mentioned previously. In that paper, the measured transmission function of the analyzer was reported. A spectrum of polycrystalline copper, acquired under the same conditions specified by Seah (Smith GC, Seah MP (1988) Surf. Interface Anal. **12**, 105-109), was presented that matched the spectrum published by Seah exceptionally well.

H. Bishop: Does the area excited by the electron probe fall within the acceptance area of the spectrometer, particularly for oblique incidence?

Author: For spectra taken with the fixed electron gun, the critical dimension for acceptance by the analyzer is 2 mm. At oblique incidence, the irradiated sample region would be essentially oval with its large axis measuring 60 μm — well under 2 mm. For spectra taken with the rotatable electron gun the critical dimension for acceptance is 20 mm. At the angle of incidence reported for this work, 60° the large axis of the oval of illumination would be ~3 mm — substantially less than 20 mm.